Does the geometry of scan bodies affect the alignment accuracy of computer-aided design in implant digital workflow: An in vitro study?

Article *in* Clinical Oral Implants Research · December 2021

DOI: 10.1111/clr.13890

5 authors, including:

James Tsoi
The University of Hong Kong

Walter Y.H. Lam
The University of Hong Kong

Zhuofan Chen
Sun Yat-Sen University

DR. YU PAN (Orcid ID : 0000-0002-9382-8530)

DR. JAMES KIT HON TSOI (Orcid ID : 0000-0002-0698-7155)

DR. EDMOND HN POW (Orcid ID : 0000-0003-2640-8437)

Article type : Original Article

Does the geometry of scan bodies affect the alignment accuracy of computer-aided design in implant digital workflow: an in vitro study?

Running title:

Accuracy of implant CAD process

Authors:

[1]Yu Pan, BDS, MDS; [1]James KH Tsoi, BSc, PhD; [1]Walter YH Lam, BDS, MDS (Pros), [2]Zhuofan Chen BDS, DDS, PhD; [1]Edmond HN Pow, BDS, MDS, PhD.

Correspondence:

Dr. Edmond HN Pow, BDS, MDS, PhD

3/F, Prince Philip Dental Hospital, 34 Hospital Road, Sai Ying Pun, Hong Kong, China.

Tel: (852) 2859 0305

Fax: (852) 2858 6114

Email: ehnpow@hku.hk

Author's institutional affiliations:

[1]Faculty of Dentistry, The University of Hong Kong, Hong Kong SAR, China.

[2]Guanghua School of Stomatology, Hospital of Stomatology, Sun Yat-sen University, Guangdong Provincial Key Laboratory of Stomatology, Guangzhou, China.

Authors' contributions:

Yu Pan: Contributed to conceptualization, methodology, investigation, manuscript preparation. James KH Tsoi: Contributed to methodology and validation. Walter YH Lam: Contributed to methodology and data analysis. Zhuofan Chen: Contributed to manuscript revision and supervision. Edmond HN Pow: Contributed to manuscript writing, reviewing, editing and supervision.

Funding statement:

There is no funding to support for this submission.

Conflict of interest disclosure:

There is no conflict of interest for this study.

Word count: 5481

Abstract

Objectives To compare 2 implant scan bodies with different geometry on the accuracy of the virtual alignment process in the digital workflow.

Materials and Methods A master model of the edentulous maxilla with 6 implants and multi-unit abutments (MUA) inserted was fabricated. Six dome-shaped and cuboidal scan bodies were mounted on the MUAs respectively and consecutively scanned by a laboratory scanner 10 times. The original scans were imported to a dental-specific CAD software and virtually aligned with the default CAD model in the implant library. Thus, 10 aligned models were created. Both the original scans and the aligned models were evaluated by an inspection software for deviation of the scan body surfaces, the centroids of scan body and MUA, the scan body centre-axis and the inter-MUA distances/angles. The two-sample T-test/Mann Whitney U test were used to analyse the data with the level of significance set at 0.05.

Results The cuboidal group showed significant greater deviations of the model surface (13.9 μm vs 10.7 μm) and the MUA centroids (31.7μm vs 22.8 μm) but smaller deviation of the inter-MUA angle (0.047° vs 0.070°) than those of the dome-shaped group ($P<0.05$). No significant differences in the deviation of scan body centroids, centre-axis and the inter-MUA distances between the 2 groups were found.

Conclusions Virtual alignment of implant scan body affected the accuracy of the digital workflow for complete-arch implant-supported prostheses (up to ~30 μm/0.09°). Different geometries of the implant scan body could also influence the transfer accuracy in the CAD process.

Mesh Keywords: dental implants, digital image processing, prosthesis design, CAD-CAM, dimensional measurement accuracy, 3-D imaging.

Introduction

Dental implants have been regarded as an optimal option for replacing missing teeth. However, the precision required for prosthesis supported by implants with external connection (59~72 μm) is much higher than the tooth-supported one (<100 μm), because dental implants are ankylosed in the alveolar bone without the periodontal ligament which serves as a cushion in the natural teeth (Kim et al., 2005; Papaspyridakos et al., 2012). In the conventional workflow, it is technically cumbersome and challenging to obtain a "passive fitting" cast implant framework (Katsoulis et al., 2017). With the advancement in CAD-CAM technology, the CAD-CAM implant framework is found promising as shown in a systematic review and the digital workflow has become popular in practice (Moris et al., 2018). The digital workflow consists of several stages including data acquisition, computer-aided design (CAD) and computer-aided manufacturing (CAM). During the stage of data acquisition, scanning could not be directly performed on an implant but through a scan body (Fluegge et al., 2017; Mizumoto et al., 2018). Currently, there are many different scan bodies in the market, varying in geometry, height, materials and surface treatments (Fluegge et al., 2017; B. Gimenez et al., 2015; Beatriz Gimenez et al., 2015; Pan et al., 2020b; Papaspyridakos et al., 2016; Pesce et al., 2018; Vandeweghe et al., 2017). After digital scanning, the CAD process follows, in which CAD files of scan body and implant are aligned with the scans by the software (Mangano et al., 2020). A 3D model will then be reconstructed for the downstream process.

The implant scan body plays an important role in the CAD stage of the digital workflow. The accuracy might be affected by the scan body's size, shape, material and surface property, which might compromise the scanning procedure and pose a negative effect on the virtual alignment process (Mizumoto et al., 2018; Pan et al., 2020a). However, few studies have investigated the transfer accuracy of implant scan bodies in the CAD process. Flugge et al.

(Fluegge et al., 2017) showed a lower precision in CAD process if a shorter and narrower scan body was used. Only 2 studies reported the deviation (15~38 μm) generated in the virtual alignment (Choi et al., 2020; Mangano et al., 2020). However, both studies performed the virtual alignment in the industrial reverse engineering software which is different from the normal clinical practice. In clinical practice, the alignment and CAD process is usually performed by the dental-specific CAD software, which is highly automatic with the algorithms, parameter settings, and accuracies never reported by the manufacturers (Tapie et al., 2015). Besides, both studies tested only one type of scan body. Therefore, further comparison on the accuracy of virtual alignment of different implant scan bodies in the CAD stage of the digital workflow is needed.

Hence, this study aimed to compare 2 implant scan bodies with different geometry on the accuracy of the virtual alignment process in the digital workflow. The null hypotheses were (1) the virtual alignment of the scan body does not create significant deviations in the digital workflow, and (2) the deviation is not significantly affected by different geometries of the implant scan body.

2. Materials and Methods

2.1 Master model preparation

Six dummy implants (NobelActive, internal RP, ø4.3/10 mm, Nobel Biocare AB, Goteborg, Sweden) were inserted in a standardized resin model of the edentulous maxilla, at the sites of lateral incisors (#12 and #22), first premolars (#14 and #24) and first molars (#16 and #26). A laboratory surveyor was used to ensure the parallelism during the site preparation. All the implants were placed at the bone level. Six multi-unit abutments (MUA) were connected with a defined torque of 30 Ncm (MUA Plus, Nobel Biocare AB).

2.2 Scan body preparation

Six dome-shaped scan bodies and 6 cuboidal scan bodies were used in this study, which were brand new and fabricated by the same manufacturer (Zfx™ Intrascan matchholder H4 and Zfx™ Evolution matchholder, Zimmer Biomet, USA) (Fig. 1). The scan body was comprised of a PEEK (poly-ether-ether-ketone) scan region (dome-shaped height 7 mm, cuboidal height 10 mm) and a titanium base (both height 4 mm). The scan bodies were inserted into the MUAs of the master model with the retaining screw tightened at 10 Ncm using a torque-controlled wrench.

2.3 Laboratory scan

A laboratory scanner from the same manufacturer was used (Zfx Evolution plus+, Zimmer Biomet, USA). The accuracy of this scanner has been evaluated in the previous study as 1~5 μm (Pan et al., 2020a). For each scan body type, the master model was consecutively scanned for 10 times (original scans). For optimization of the post-processing, the original scans were carefully inspected for any noises and incomplete surfaces. If the scan region of the scan body was not acquired completely, an additional scan would be performed. All original scans were exported as standard triangulation language (STL) files.

2.4 Virtual alignment

The original scan of the scan body (Fig. 2a) was first imported into the dental-specific CAD software (EXOCAD, Woburn, MA, USA). The CAD model from the implant library was superimposed onto each scan body one after another (Fig. 2b) according to a two-step alignment protocol incorporated in the software: first, a coarse matching of the 2 surfaces (original VS CAD) was performed through manual recognition of the geometric features on the scan body. Second, the automatic computation was implemented to achieve "best fit" between the surfaces. The alignment procedure was performed once for each scan body in the original scan. The aligned model (Fig. 2c) was then exported into a single STL file. A total of 10 aligned models for each group were created for further analyses.

2.5 Establishing geometric features of the scan body

The original scans and aligned models were imported into an inspection software (Geomagic Control 2014, Geomagic, Morrisville, USA). Three geometric features were virtually established on each scan body for further 3D analyses: the centroids of the scan body and MUA represent the position of the implant scan body and the implant abutment, respectively. The centre-axis of the scan body represents the orientation of the underlying dental implant. The features were established based on the following protocol according to the ISO 17450-1-2-3 guidelines:

- Trim the model: the base part, including the palate and alveolar ridge, was trimmed. Every model was segmented into 6 parts with each included a single scan body.
- Define the top plane: the top surface of scan body was captured and then defined as the top plane using the least-squares (Lsq) algorithm.
- Define the centre-axis: the axial surfaces of the scan body were captured to compute the centre-axis.
- Define the MUA plane: For the original scan, the top plane was projected in the negative

Z-direction along the centre-axis of the scan body for a distance corresponding to the height of the scan body (cuboidal: 14 mm, dome-shaped: 11 mm). For the aligned model, the MUA plane was directly established on the bottom plane of the virtual MUA (Fig.3).

- Define the centroids: the centroids of the scan body and MUA were established by intersecting the centre-axis with the top plane and the MUA plane.

2.6 Repeatability of geometric features

For the original scans and aligned models, the scan bodies' geometric features were repeatedly captured on the same model for 5 times to determine the repeatability of this protocol. The distance between the centroids and angles between the centre-axes were measured and calculated as mean and SD.

2.7 3D comparisons

Each scan body in the original scan (reference) was superimposed on the corresponded aligned model (test) using the iterative-closest-points (ICP) criteria (Fig.4). This protocol ensured the same 3D coordinate system was used in the inspection software when the difference between the scan body in an original scan and its aligned model was measured. The surface deviation of the scan body (root-mean-square, RMS) was then computed and demonstrated by a colour map. The Euclidean distance ($\Delta 3D$) of the centroids, the related linear deviation in three directions (ΔX, ΔY, and ΔZ), and the angular deviation of the centre-axes ($\Delta\alpha$) between the original scans and aligned models were measured. Inter-MUA distance and angulations, which were defined as the distance and angulation between the adjacent MUA centroids and centre-axes, at different sites (#16-14, #14-12, #12-22, #22-24, #24-#26, #16-26), were measured respectively (Fig.5). The difference in the inter-MUA distance/angulation between the original scans and aligned model was evaluated.

2.8 Statistical analyses

A pilot study was conducted to with 3 scans in each group. T-test showed a large effect size (f=0.994) for the difference in deviation of the MUA centroid between the two scan bodies. The sample size was then calculated using G*power (Heinrich Heine, Universität Düsseldorf, Germany) with a power of 90% at an α-level of 0.05 (two-tailed), indicating at least 4 scans per group were needed.

Normality and equivalence of variance of the data were evaluated by the Shapiro-Wilk test and Levene's test, respectively. Mann Whitney U test was performed to compare the inter-group Δ3D and Δα (dome-shaped vs cuboidal scan body). Two-way ANOVA was conducted to evaluate the effect of site and geometry on deviation of inter-MUA distance/angulation. Subgroup comparisons were performed by Two-sample T-test and One-way ANOVA, followed by multiple comparisons by Tuckey/Dunnett's T3 test. The Wilcoxon Signed Rank Test was conducted for intra-group comparisons between Δ3D of scan body centroid and MUA centroid. One-way Friedman's ANOVA was performed for intra-group comparisons of ΔX, ΔY, and ΔZ of the MUA centroid. The analyses were implemented by SPSS 24.0 (IBM SPSS software; IBM Corporation, Cary, NC, USA). The level of significance was set at 0.05.

Ethics approval was not required for this in vitro study. A modified CONSORT checklist for reporting in vitro study was used as quality assessment of this study.

3. Results

3.1 Repeatability of geometric features establishment

The linear deviation between the centroids and angular deviation between the centre-axes of the scan bodies in the original scans and aligned models was less than 0.8 μm/0.05° and 0.001 μm/0.001°, respectively.

3.2 Surface deviations

The deviations ranged from 13.1 to 15.3 μm and 10.3 to 11.1 μm in the cuboidal and dome-shaped groups, respectively. The Shapiro-Wilk test indicated that the data conformed to a normal distribution. Equal of variance was assumed. The deviations of the dome-shaped group (mean 10.7 μm, SD 0.2) was significantly less than that of the cuboidal group (mean 13.9 μm, SD 0.7) (t =-25.037, $p<0.001$). The colour maps indicated the surface deviations between the original scan and the aligned model. High deviations were found at the margin of the scan region and curved surfaces (Fig.6~7).

3.3 Deviation of the geometric features

The results of Δ3D, ΔX, ΔY and ΔZ of the centroids were shown in Fig. 8 and Table 1. The Δ3D of the scan body's centroid ranged from 4.3 to 31.3 μm, while that of the MUA's centroid ranged from 9.5 to 52.6 μm. The Δα of the centre-axis ranged from 0.006 to 0.257°. The Shapiro-Wilk test indicated that the data did not conform to a normal distribution. The pooled data of 2 scan body groups showed that the median Δ3D of the MUA centroids (median 26.9 μm, IQR 16.9-32.7) was significantly greater than that of the scan body centroids (median 12.6 μm, IQR 10.8-24.4, Z=-8.778, $p<0.001$).

No significant difference in Δ3D of the scan body's centroid was found between the 2 scan bodies (cuboidal median 14.6, IQR 9.1-27.5, dome-shaped median 12.2, IQR 11.4-19.0,

Z=-0.682, p=0.495) (Fig. 8). The ΔX and ΔY were comparable between 2 groups, while significant greater ΔZ was noticed in the dome-shaped group compared to the Cuboidal group (Z=5.882, p<0.001). Within the cuboidal group, the ΔZ was significantly less than ΔX (Z=4.002, p<0.001) and ΔY (Z=4.518, p<0.001), while within the dome-shaped group, ΔY was significantly less than ΔX (Z=4.441, p<0.001) and ΔZ (Z=-3.213, p=0.004) (Table 1).

The Δ3D of the MUA centroids of the cuboidal group (median 31.7 μm, IQR 18.6-35.1) was significantly greater than the dome-shaped group (median 22.8 μm, IQR 14.9-28.4) (Fig. 6, Z=-3.501, p<0.001). The ΔY of the cuboidal group was significantly greater than the dome-shaped group (Z=-5.419, p<0.001).

No significant differences in Δα of the centre-axes of the scan body were found between 2 groups (cuboidal median 0.088°, IQR 0.030-0.108, dome-shaped median 0.085°, IQR 0.068-0.108, Z=-1.688, p=0.091).

3.4 Deviation of inter-MUA distance and angulation

Deviations of the inter-MUA distance and angulation of the aligned models were shown in Table 1. The Shapiro-Wilk test indicated that the data conformed to a normal distribution. Equal of variance was not assumed. Deviation of inter-MUA distance/angulation ranged from 0.6 to 49.3 μm /0.001 to 0.215° and 0.9 to 31.9 μm/0.001 to 0.339° in the cuboidal and dome-shaped group, respectively.

The deviation of inter-MUA angulation of the cuboidal group was significantly less than the dome-shaped (F=9.607, p=0.002). No significant difference in the overall deviation of inter-MUA distance was found between 2 scan bodies (F=0.523, p=0.473). However, site-specific differences were found (F=4.894, p=0.001). At the site #12-22, the mean deviation of the cuboidal group was significantly greater than the dome-shaped group

(t=8.063, $p<0.001$). On the contrary, at site #24-26, the mean deviation of the dome-shaped group was significantly greater than the cuboidal group (t=-9.597, $p<0.001$).

4. Discussion

Although data acquisition is essential in the digital, data processing is equally crucial but seldom studied workflow (Choi et al., 2020; Koch et al., 2016; Mangano et al., 2020; Mizumoto et al., 2018; Vandeweghe et al., 2017). In the present study, we quantified the deviation produced in the CAD process when the scanned digital data were matched with the implant library data. The mean surface deviation of the scan body (13.9 μm) and the median Δ3d of MUA centroid (31.7 μm) were comparable to those found in previous studies (Choi et al., 2020; Mangano et al., 2020). Our results also showed the deviation of the inter-MUA distance and angulation in a multi-implant scenario was up to 15.7 μm and 0.070° respectively and that have never been reported in any previous studies. Therefore, the first null hypothesis was rejected. Although the deviations created in the CAD process seemed to be small and clinically insignificant, they would propagate to the downstream of the digital workflow and contribute to the total error of the definitive prostheses. Besides, we found different geometries of scan bodies could create different levels of deviation during the virtual alignment procedure. The dome-shaped group showed significantly higher accuracy in terms of the scan body surface, the scan body centroid and the MUA centroid than the cuboidal group. Hence, the second null hypothesis was also rejected.

Our results showed that the accuracies of 2 tested scan bodies during the virtual alignment process were different. Regarding the deviations in the X-, Y-, Z-dimensions, a significant greater ΔY was noticed in the cuboidal scan body (27.8 μm) compared to that of the dome-shaped one (7.4 μm), suggesting that scan body geometry could significantly affect the horizontal discrepancy. The horizontal misfits would lead to stress concentrations in abutment screws, framework and peri-implant bone, and that could jeopardize the survival of implant prostheses (Pan et al., 2020a; Spazzin et al., 2011).

The deviations of the scan body centroids were significantly less than those of the MUA centroids, which is not unexpected. Since the virtual MUA position was computed based on the scan body projecting along its centre-axis in the negative Z-direction, the error would be magnified if the centre-axis was misaligned (Del Corso et al., 2009) (Chia et al., 2017). Hence, accuracy measurement should not be undertaken at the scan body level only as this might underestimate the actual deviation degree at the MUA level.

Although both scan bodies showed comparable deviations in the inter-MUA distance of the aligned models (~15 μm), distribution of the deviations within the arch was different. It could be due to the systematic error on the focal plane setting of the scanner (Patzelt et al., 2014; Seitz et al., 1993). This uneven distribution of the deviation is unfavourable, which may cause misfits between the implant/abutment and the superstructure (Jokstad et al., 2015). Therefore, it might be beneficial to set the scanner's focal plane at the centre of the model, and thereby the scanning deviations would be evenly distributed.

In this study, the two scan bodies showed a comparable degree of angular error for single site, while the cuboidal scan body showed a significant higher accuracy in inter-MUA angulation. It could be due to the length of the cuboidal scan body which is longer (10 mm) than the dome-shaped one (7 mm), which can better indicate the implant orientation. Previous clinical studies suggested that the maximum acceptable angular error between 2 implants of around 15 mm long should not exceed 0.4° (Rutkunas et al., 2017). However, for a shorter implant (10mm) and MUA (height 2.5 mm) used in the present study, an angular deviation up to 0.459° might still be acceptable, based on the formula: 2 ×

$\tan^{-1}(\frac{0.05}{L}) \times 180/\boldsymbol{\pi}$, the maximum movement (50 μm) of dental implant, L=implant + abutment length in mm (Andriessen et al., 2014). Hence, both scan bodies tested (mean 0.09°, maximum 0.257°) seem to be clinically acceptable in this respect.

There are many factors affecting the accuracy during CAD processing. Manufacturing tolerance is one of them as the size of any commercial scan body (output) inevitably varies to a certain degree from its corresponding CAD library (input). In this study, it was not measured directly and hence how much the deviation of the aligned model derived from the scan body tolerance could not be determined. However, we had measured the surface deviations of the individual scan body (10~14 μm), which was a combined error of both the tolerance and the scanning accuracy. In our previous works, scanning accuracy of the laboratory scanner used in this study has been verified as 1~5 μm (Pan et al., 2020a). Therefore, we could assume the tolerance of the scan body to be ~9 μm. This result is slightly greater than that reported by another study (4~7 μm) but of comparable size (<10 μm) (Chia et al., 2017). Most manufacturers do not specify the precision of their scan bodies. Only one recent study reported that the scan body tolerance of 2~25 μm might lead to 50 ~130 μm of deviation of the virtual implant position, which was significantly higher than this study (22~30 μm) (Schmidt et al., 2019). It suggests that the manufacturing tolerance of scan body could play an essential role in the transfer accuracy of implant position in the digital workflow.

Inaccurate scanning may lead to incorrect matching of the scan body and distort the final virtual model (Vandeweghe et al., 2017). Scanning accuracy relies on point clouds' quality, which is determined by the light signals project and return from the scanned surfaces (Del Corso et al., 2009). Then a question is raised: would the shape of scan body affect the scanning accuracy? It has been reported that the precision of extraoral scanning of scan bodies depends on the scan body surface design as well as its geometry (Fluegge et al., 2017). In this study, we used a dome-shaped scan body consisted of complicated curve surfaces, and a cuboidal scan body comprised simple and straight asymmetry surfaces with sharp edges. The results showed that the dome-shaped group achieved less surface deviation, which might be due to the rounded edges and smooth surfaces (Gonzalez de Villaumbrosia et al., 2016). On the contrary, sharp features might make significant noise in the data that could not be handled by most post-processing algorithms (Rudolph et al., 2002; Wang et al., 2013). Surface contour of the scanned object also plays an essential role in virtual alignment process (Bernardini et al., 2002). It has been suggested that distinctive points with high curvature is the key for the first step (initial recognition), while the second step (refined matching) can be achieved by the smooth areas (Rodolà et al., 2015). Although both types of scan body used in this study have smooth regions, only the dome-shaped one has pronounced curvatures, preventing two aligned surfaces from sliding relative to each other during the matching procedure (Bernardini et al., 2002).

Few details could be found regarding how the virtual alignment was performed in previous studies. Two studies that investigate the alignment accuracy, however, used reverse engineering software with the ICP algorithm and pre-set parameters, instead of the dental-specified software that used in the clinical practice, of which the point clouds sampling and tolerance setting are unknown (Choi et al., 2020; Mangano et al., 2020). Theoretically, a greater amount of point sampling plus a tighter tolerance can result in a better alignment. However, this will prolong the processing time (Rodolà et al., 2015). In the present study, the alignment deviations were based on one of the most commonly used dental-specific software (EXOCAD), which made the results more clinically relevant although its parameters are unknown and could not be compared with other engineering software.

To eliminate the errors in the virtual alignment, the design of CAD model in the implant library is also important. The cuboidal one consisted of 4 separated rectangular planes only, without definite line angles and corners which could interfere with the matching accuracy. For the dome-shaped one, the CAD model is designed deliberately shorter than the scan region of the physical scan body, because the areas near the digital model boundary were easily distorted. Thus, only reliable point clouds from the surface are included for matching (Bernardini et al., 2002). Therefore, the designs of both cuboidal and dome-shaped CAD models appear to be appropriate.

Therefore, we propose the designs of an implant scan body should be of rounded edges, high curvature, and smooth surfaces with an asymmetrical feature. The designs of the implant library should be dimensionally identical to the physical scan body, while features difficult for scanning, especially sharp edges and boundaries, should be excluded.

There are some limitations in the present study. First, the small deviation found in this study (20~30 μm) could be due to the use of precise laboratory scanner in a well-controlled experimental environment, with most of the potential deleterious factors at the chairside eliminated. Hence, the "real" deviations created by intraoral scanners (IOS) in the clinical situations might be underestimated. Second, only cuboidal and dome-shaped scan bodies were investigated in this study. They were used because they were made by the same manufacturer with the same materials, structure (base height and screw design), surface treatment, and manufacturing tolerance. Therefore, such potential confounding factors were largely eliminated. Although the results cannot be extrapolated to the scan bodies of another brand, design, and material, this study highlighted the implant scan body's vital role in scanning accuracy, and the findings are not only important to clinicians and dental technicians but also the researchers and engineers for further development of scan bodies. Finally, in this study, the repeatability of the alignment process was not investigated although a similar previous study reported that it was insignificant at 0.3~1.1 μm (Choi et al., 2020).

Conclusions

Within the limitations of this *in vitro* study, the following conclusions were drawn:

1. The virtual alignment process of the implant scan body could affect the accuracy of the virtual model in the digital workflow of complete-arch implant-supported prostheses (up to 30 μm deviation of the implant position).
2. Different geometries of the implant scan body could influence the transfer accuracy in the digital workflow.

Figure legend

Fig.1 Dome-shaped and cuboidal scan bodies.

Fig. 2 Original (a) and CAD (b) models of the scan body were superimposed and an aligned model was created (c).

Fig. 3 Geometric features were established on the aligned model.

Fig.4 Original model (a) was superimposed on the aligned model (b) and the linear and angular deviation were measured (c).

Fig.5 The distances between adjacent MUA centroids were measured.

Fig.6 The color map of the dome-shaped scan body.

Fig.7 The color map of the cuboidal scan body.

Fig.8 Δ3D deviation of the scan body and MUA centroids in the cuboidal group and dome-shaped group. *** Wilcoxon Signed Rank test, $p<0.001$.

References

Andriessen, F. S., Rijkens, D. R., van der Meer, W. J., & Wismeijer, D. W. (2014). Applicability and accuracy of an intraoral scanner for scanning multiple implants in edentulous mandibles: a pilot study. *Journal of Prosthetic Dentistry, 111*(3), 186-194. http://doi.org/10.1016/j.prosdent.2013.07.010

Bernardini, F., & Rushmeier, H. (2002). The 3D Model Acquisition Pipeline. *21*(2), 149-172. http://doi.org/10.1111/1467-8659.00574

Chia, V. A., Esguerra, R. J., Teoh, K. H., Teo, J. W., Wong, K. M., & Tan, K. B. (2017). In Vitro Three-Dimensional Accuracy of Digital Implant Impressions: The Effect of Implant Angulation. *International Journal of Oral and Maxillofacial Implants, 32*(2), 313-321. http://doi.org/10.11607/jomi.5087

Choi, Y.-D., Lee, K. E., Mai, H.-N., & Lee, D.-H. (2020). Effects of scan body exposure and operator on the accuracy of image matching of implant impressions with scan bodies. *The Journal of prosthetic dentistry*. http://doi.org/10.1016/j.prosdent.2020.04.004

Del Corso, M., Aba, G., Vazquez, L., Dargaud, J., & Dohan Ehrenfest, D. M. (2009). Optical three-dimensional scanning acquisition of the position of osseointegrated implants: an in vitro study to determine method accuracy and operational feasibility. *Clinical Implant Dentistry and Related Research, 11*(3), 214-221. http://doi.org/10.1111/j.1708-8208.2008.00106.x

Fluegge, T., Att, W., Metzger, M., & Nelson, K. (2017). A Novel Method to Evaluate Precision of Optical Implant Impressions with Commercial Scan Bodies—An Experimental Approach. *Journal of Prosthodontics, 26*(1), 34-41. http://doi.org/10.1111/jopr.12362

Gimenez, B., Ozcan, M., Martinez-Rus, F., & Pradies, G. (2015). Accuracy of a Digital Impression System Based on Active Triangulation Technology With Blue Light for Implants: Effect of Clinically Relevant Parameters. *Implant Dentistry, 24*(5), 498-504. http://doi.org/10.1097/id.0000000000000283

Gimenez, B., Ozcan, M., Martinez-Rus, F., & Pradies, G. (2015). Accuracy of a Digital Impression System Based on Active Wavefront Sampling Technology for Implants Considering Operator Experience, Implant Angulation, and Depth. *Clinical Implant Dentistry and Related Research, 17*(1), e54-e64. http://doi.org/10.1111/cid.12124

Gonzalez de Villaumbrosia, P., Martinez-Rus, F., Garcia-Orejas, A., Salido, M. P., & Pradies, G. (2016). In vitro comparison of the accuracy (trueness and precision) of six extraoral dental scanners with different scanning technologies. *Journal of Prosthetic Dentistry, 116*(4), 543-550.e541. http://doi.org/10.1016/j.prosdent.2016.01.025

Jokstad, A., & Shokati, B. (2015). New 3D technologies applied to assess the long-term clinical effects of misfit of the full jaw fixed prosthesis on dental implants. *Clinical Oral Implants Research, 26*(10), 1129-1134. http://doi.org/10.1111/clr.12490

Katsoulis, J., Takeichi, T., Gaviria, A. S., Peter, L., & Katsoulis, K. (2017). Misfit of implant prostheses and its impact on clinical outcomes. Definition, assessment and a systematic review of the literature. *European Journal of Oral Implantology, 10*(suppl1), 121-138. http://doi.org/10.7892/boris.110976

Kim, Y., Oh, T.-J., Misch, C. E., & Wang, H.-L. (2005). Occlusal considerations in implant therapy: clinical guidelines with biomechanical rationale: Occlusal consideration in implant therapy. *Clinical Oral Implants Research, 16*(1), 26-35. http://doi.org/10.1111/j.1600-0501.2004.01067.x

Koch, G. K., Gallucci, G. O., & Lee, S. J. (2016). Accuracy in the digital workflow: From data acquisition to the digitally milled cast. *The Journal of Prosthetic Dentistry, 115*(6), 749-754. http://doi.org/10.1016/j.prosdent.2015.12.004

Mangano, F., Lerner, H., Margiani, B., Solop, I., Latuta, N., & Admakin, O. (2020). Congruence between Meshes and Library Files of Implant Scanbodies: An In Vitro Study Comparing Five Intraoral Scanners. *Journal of clinical medicine, 9*(7), 2174. http://doi.org/10.3390/jcm9072174

Mizumoto, R. M., & Yilmaz, B. (2018). Intraoral scan bodies in implant dentistry: A systematic review. *Journal of Prosthetic Dentistry, 120*(3), 343-352. http://doi.org/10.1016/j.prosdent.2017.10.029

Moris, I. C. M., Monteiro, S. B., Martins, R., Ribeiro, R. F., & Gomes, E. A. (2018). Influence of Manufacturing Methods of Implant-Supported Crowns on External and Internal Marginal Fit: A Micro-CT Analysis. *Biomed Research International*. http://doi.org/10.1155/2018/5049605

Pan, Y., Tam, J. M. Y., Tsoi, J. K. H., Lam, W. Y. H., Huang, R., Chen, Z., & Pow, E. H. N. (2020a). Evaluation of laboratory scanner accuracy by a novel calibration block for complete-arch implant rehabilitation. *Journal of Dentistry, 102*, 103476. http://doi.org/https://doi.org/10.1016/j.jdent.2020.103476

Pan, Y., Tam, J. M. Y., Tsoi, J. K. H., Lam, W. Y. H., & Pow, E. H. N. (2020b). Reproducibility of laboratory scanning of multiple implants in complete edentulous arch: Effect of scan bodies. *Journal of Dentistry, 96*, 103329. http://doi.org/10.1016/j.jdent.2020.103329

Papaspyridakos, P., Benic, G. I., Hogsett, V. L., White, G. S., Lal, K., & Gallucci, G. O. (2012). Accuracy of implant casts generated with splinted and non-splinted impression techniques for edentulous patients: an optical scanning study. *Clinical Oral Implants Research, 23*(6), 676-681. http://doi.org/10.1111/j.1600-0501.2011.02219.x

Papaspyridakos, P., Gallucci, G. O., Chen, C. J., Hanssen, S., Naert, I., & Vandenberghe, B. (2016). Digital versus conventional implant impressions for edentulous patients: accuracy outcomes. *Clinical Oral Implants Research, 27*(4), 465-472. http://doi.org/10.1111/clr.12567

Patzelt, S., Emmanouilidi, A., Stampf, S., Strub, J., & Att, W. (2014). Accuracy of full-arch scans using intraoral scanners. *Clin Oral Invest, 18*(6), 1687-1694. http://doi.org/10.1007/s00784-013-1132-y

Pesce, P., Pera, F., Setti, P., & Menini, M. (2018). Precision and Accuracy of a Digital Impression Scanner in Full-Arch Implant Rehabilitation. *International Journal of Prosthodontics, 31*(2), 171-175. http://doi.org/10.11607/ijp.5535

Rodolà, E., Albarelli, A., Cremers, D., & Torsello, A. (2015). A simple and effective relevance-based point sampling for 3D shapes. *Pattern Recognition Letters, 59*, 41-47. http://doi.org/10.1016/j.patrec.2015.03.009

Rudolph, H., Quaas, S., & Luthardt, R. G. (2002). Matching point clouds: limits and possibilities. *International Journal of Computerized Dentistry, 5*(2-3), 155-164.

Rutkunas, V., Geciauskaite, A., Jegelevicius, D., & Vaitiekunas, M. (2017). Accuracy of digital implant impressions with intraoral scanners. A systematic review. *Eur J Oral Implantol, 10* (Suppl 1), 101-120.

Schmidt, A., Billig, J. W., Schlenz, M. A., Rehmann, P., & Wostmann, B. (2019). Influence of the Accuracy of Intraoral Scanbodies on Implant Position: Differences in Manufacturing Tolerances. *International Journal of Prosthodontics, 32*(5), 430-432. http://doi.org/10.11607/ijp.6371

Seitz, G., & Tiziani, H. J. (1993). Resolution limits of active triangulation systems by defocusing. *Optical Engineering, 32*(6), 1374-1383. http://doi.org/10.1117/12.133241

Spazzin, A. O., Abreu, R. T., Noritomi, P. Y., Consani, R. L., & Mesquita, M. F. (2011). Evaluation of stress distribution in overdenture-retaining bar with different levels of vertical misfit. *Journal of Prosthodontics, 20*(4), 280-285. http://doi.org/10.1111/j.1532-849X.2011.00708.x

Tapie, L., Lebon, N., Mawussi, B., Fron Chabouis, H., Duret, F., & Attal, J. P. (2015). Understanding dental CAD/CAM for restorations--the digital workflow from a mechanical engineering viewpoint. *International Journal of Computerized Dentistry, 18*(1), 21-44.

Vandeweghe, S., Vervack, V., Dierens, M., & De Bruyn, H. (2017). Accuracy of digital impressions of multiple dental implants: an in vitro study. *Clinical Oral Implants Research, 28*(6), 648-653. http://doi.org/10.1111/clr.12853

Wang, J., Yu, Z., Zhu, W., & Cao, J. (2013). Feature - Preserving Surface Reconstruction From Unoriented, Noisy Point Data. *Computer Graphics Forum, 32*(1), 164-176. http://doi.org/10.1111/cgf.12006

Table 1 Deviations of the scan body and MUA centroid and inter-MUA distance after virtual alignment.

	Cuboidal	Dome-shaped	*p*	*df*	*t/Z*
Linear deviation of Scan body centroid (μm/median (IQR))					*Z**
3D	14.6 (9.1-27.5)	12.2 (11.4-19.0)	0.495	118	-0.682
$\|X\|$	8.8 (3.5-12.6) [a]	8.0 (5.1-14.6) [a]	0.275	118	1.092
$\|Y\|$	6.5 (3.1-24.8) [a]	6.4 (2.7-11.7) [a]	0.485	118	-0.698
$\|Z\|$	1.2 (0.7-3.6) [b]	7.5 (4.4-8.7) [a]	<0.001	118	5.882
Linear deviation of MUA centroid (μm/median (IQR))					
3D	31.7 (18.6-35.1)	22.8 (14.9-28.4)	<0.001	118	-3.501
$\|X\|$	15.3 (4.8-36.4) [a]	15.4 (8.1-27.1) [a]	0.861	118	-0.175
$\|Y\|$	27.8 (11.2-31.1) [b]	7.4 (4.3-11.7) [b]	<0.001	118	-5.419
$\|Z\|$	2.9 (1.4-4.3) [c]	6.3 (3.2-8.1) [b]	<0.001	118	3.450

Angular deviation of scan body centre axis (°/median (IQR))	0.088 (0.030-0.108)	0.085 (0.068-0.108)	0.091	118	1.688
Inter-MUA distance (μm/mean (SD))					$t^{\#}$
16-14	8.3 (9.7) [a]	19.1 (7.9) [a,c]	0.090	18	-1.932
14-12	11.0 (4.1) [a]	17.9 (5.8) [a,b,c]	0.060	18	-2.184
12-22	39.4 (7.8) [b]	6.4 (4.8) [b]	<0.001	18	8.063
22-24	16.6 (6.2) [a]	16.0 (9.5) [a,b]	0.250	18	1.236
24-26	4.8 (2.9) [a]	27.7 (4.5) [c]	<0.001	18	-9.597
16-26	7.1 (2.1) [a]	11.9 (7.9) [a,b]	0.230	18	-1.292
Total	14.6 (6.7)	15.7 (7.1)	0.690	118	-0.402
Inter-MUA angulation (°/mean (SD))					$t^{\#}$

16-14	0.021(0.023) [a,b]	0.075(0.034) [a]	0.001	18	-4.169
14-12	0.022(0.013) [a,b]	0.062(0.043) [a]	0.011	10	-2.817
12-22	0.027(0.026) [a,b]	0.085(0.044) [a]	0.002	18	-3.552
22-24	0.017(0.008) [a]	0.075(0.097) [a]	0.075	18	-1.889
24-26	0.039(0.009) [b]	0.031(0.021) [a]	0.301	12	1.080
16-26	0.158(0.028) [c]	0.092(0.048) [a]	0.001	18	3.784
Total	0.047(0.054)	0.070(0.055) [a]	0.024	118	0.761

Distribution of distortions in column that do not share the same letters are significant difference.

* Mann-Whitney U test

Two-sample T-test

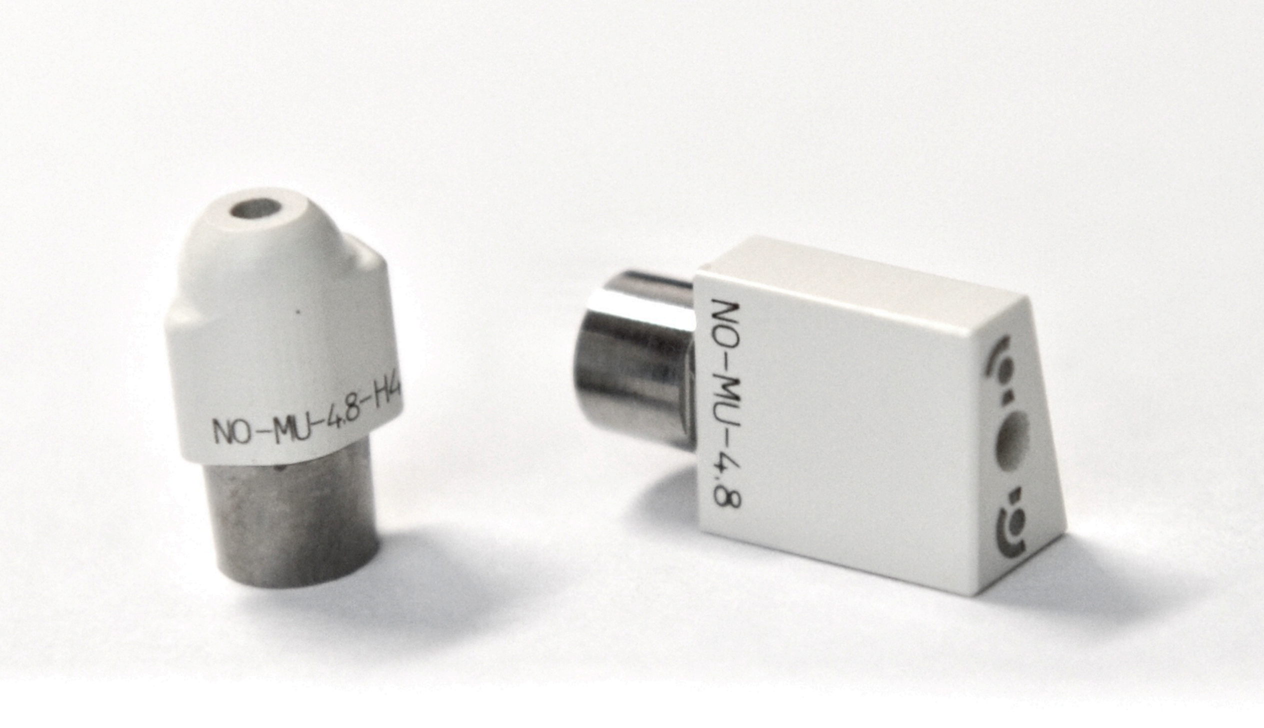
NO-MU-4.8-H4
NO-MU-4.8

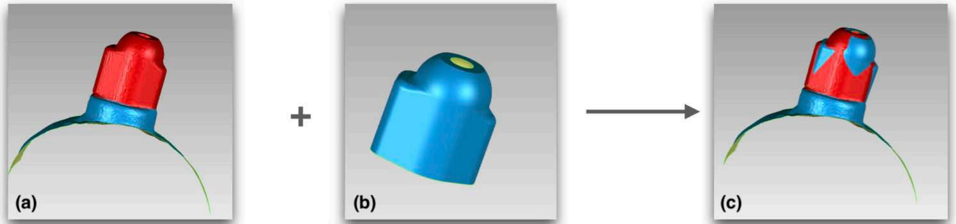
(a)
+
(b)
(c)

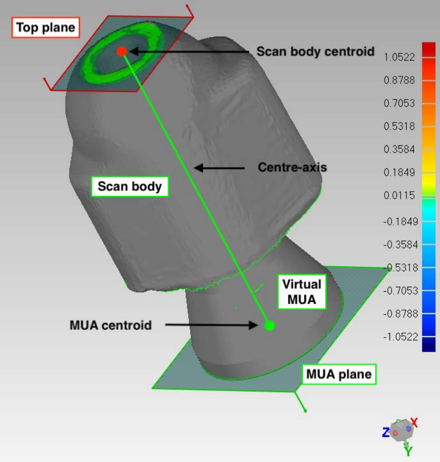
Top plane
Scan body centroid
Centre-axis
Scan body
Virtual MUA
MUA centroid
MUA plane
1.0522
0.8788
0.7053
0.5318
0.3584
0.1849
0.0115
-0.1849
-0.3584
-0.5318
-0.7053
-0.8788
-1.0522
Z
X
Y

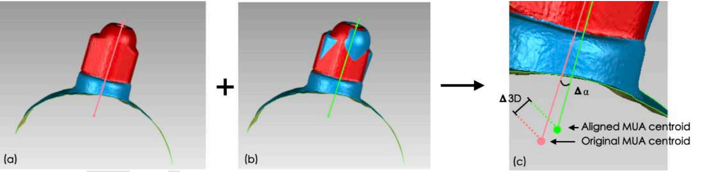

(a)
(b)
(c)
Δ 3D
Δ α
Aligned MUA centroid
Original MUA centroid

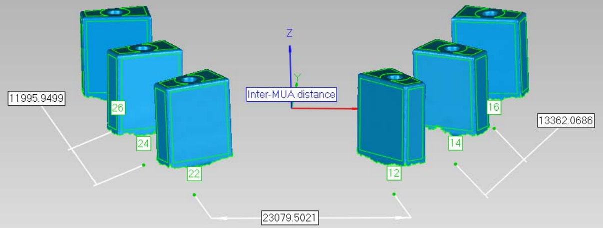
Z
Y
Inter-MUA distance
11995.9499
26
24
22
12
14
16
13362.0686
23079.5021

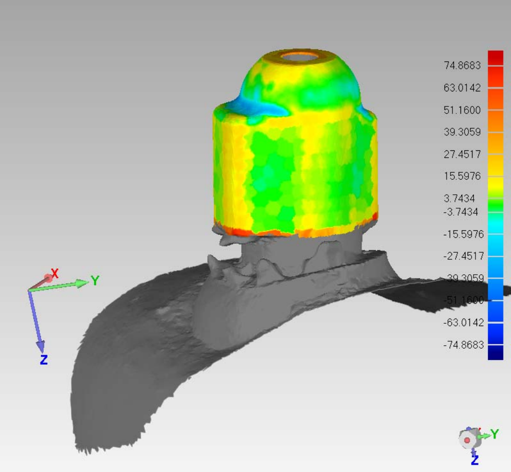

74.8683
63.0142
51.1600
39.3059
27.4517
15.5976
3.7434
-3.7434
-15.5976
-27.4517
-39.3059
-51.1600
-63.0142
-74.8683
X
Y
Z

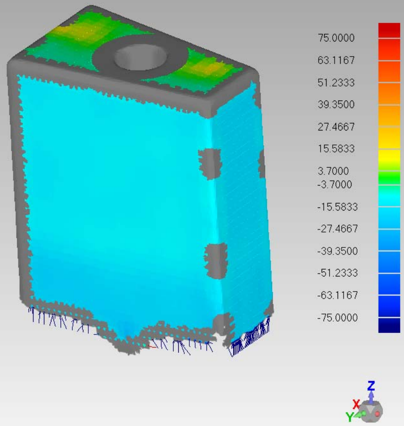

75.0000
63.1167
51.2333
39.3500
27.4667
15.5833
3.7000
-3.7000
-15.5833
-27.4667
-39.3500
-51.2333
-63.1167
-75.0000
Z
X
Y

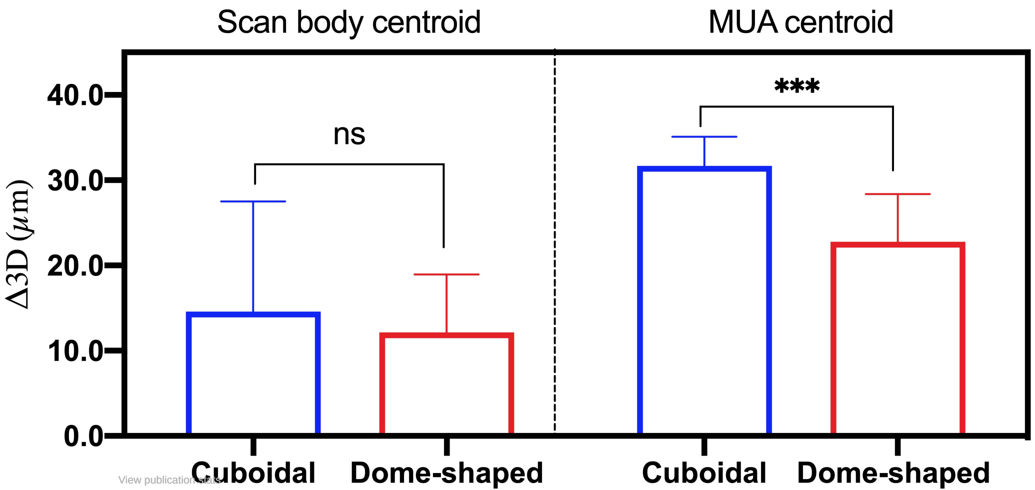
Scan body centroid
MUA centroid
ns
***
Δ3D (μm)
40.0
30.0
20.0
10.0
0.0
Cuboidal
Dome-shaped
Cuboidal
Dome-shaped